Lessons from the first Magnetar Wind Nebula

Jonathan Granot

Open University of Israel

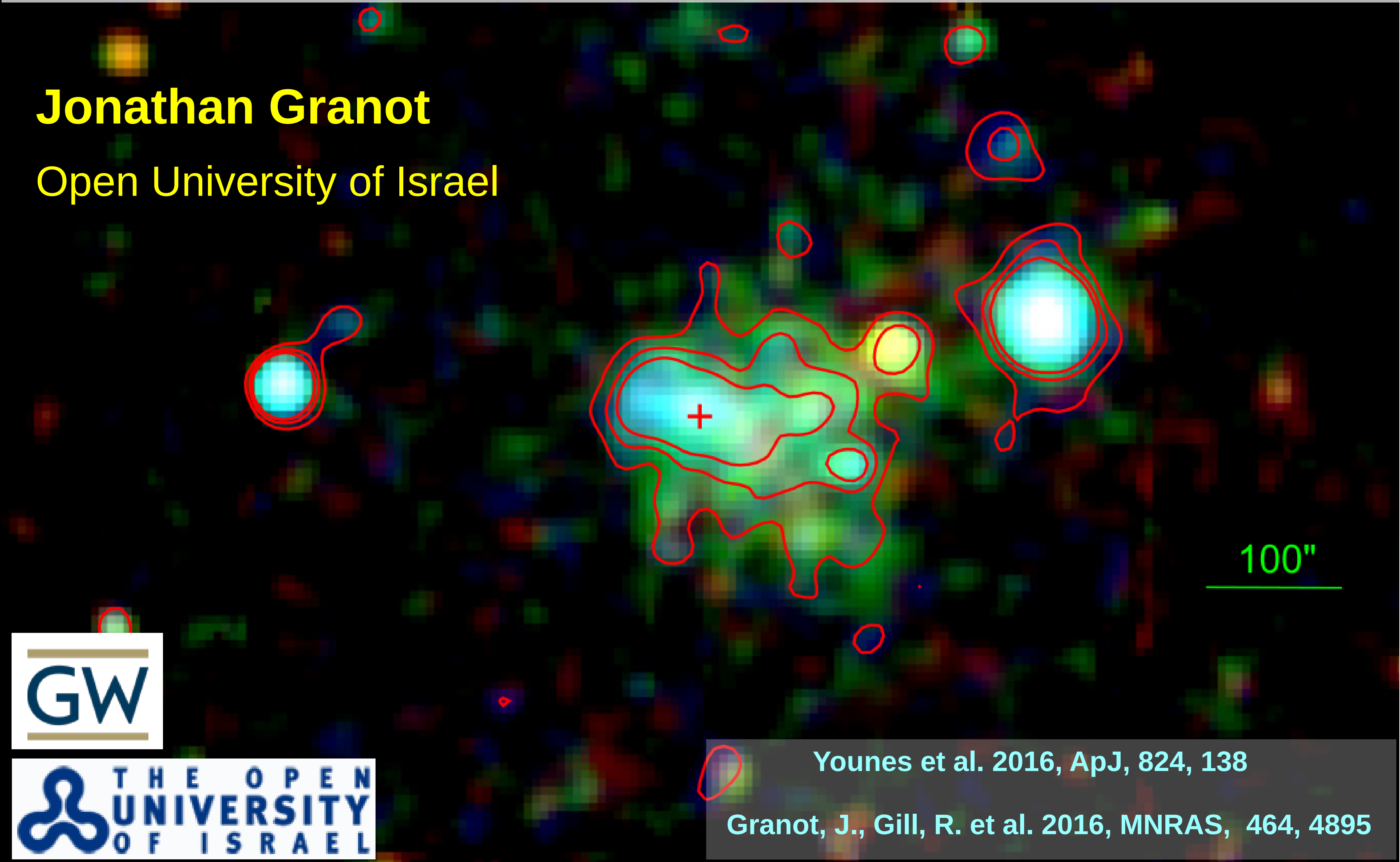

Younes et al. 2016, ApJ, 824, 138

Granot, J., Gill, R. et al. 2016, MNRAS, 464, 4895

High Energy Astrophysics Workshop, February 28, 2017 Jerusalem

Outline of the Talk:

- **Introduction**: magnetars & Pulsar Wind Nebulae
- **Observations**: the 1st MWN discovered around Swift J1834.9−0846
- Association with SNR W41 & MWN detectability
- **GeV/TeV Source**: next talk by Ramandeep Gill
- **Dynamics** of the Nebula + SNR – two main dynamical regimes
- **Internal Structure** of the Nebula: ideal MHD ➔ non-ideal low-σ flow
- X-ray synchrotron Nebula **Size**: electron advection, diffusion, cooling
- Steady-state X-ray emission: **energy balance** ➔ $\dot{E}_{rot}$ is insufficient
- Alternative **energy source**: magnetar's B-field decay
- Conclusions

Magnetars: differences from "normal" pulsars

Compared to "normal" radio pulsars, magnetars have:

- Long rotation periods: $P \approx 2 - 12\ \mathrm{s}$
- Large period derivatives: $\dot{P} \sim 10^{-13} - 10^{-10}$
- Small spin-down ages

$$\dot{P} \propto P^{2-n} \qquad P(t) = P_0 \left(1 + \frac{t}{t_0}\right)^{1/(n-1)}$$

$$t \approx \frac{P}{(n-1)\dot{P}} \equiv \tau_c \qquad (P_0 \ll P)$$

- Lower spin-down power

$$L_{\rm sd} = -I\Omega\dot{\Omega} = \frac{4\pi^2 I \dot{P}}{P^3} \sim 10^{30} - 10^{34}\ \mathrm{erg\ s^{-1}}$$

- Higher inferred dipole surface magnetic fields

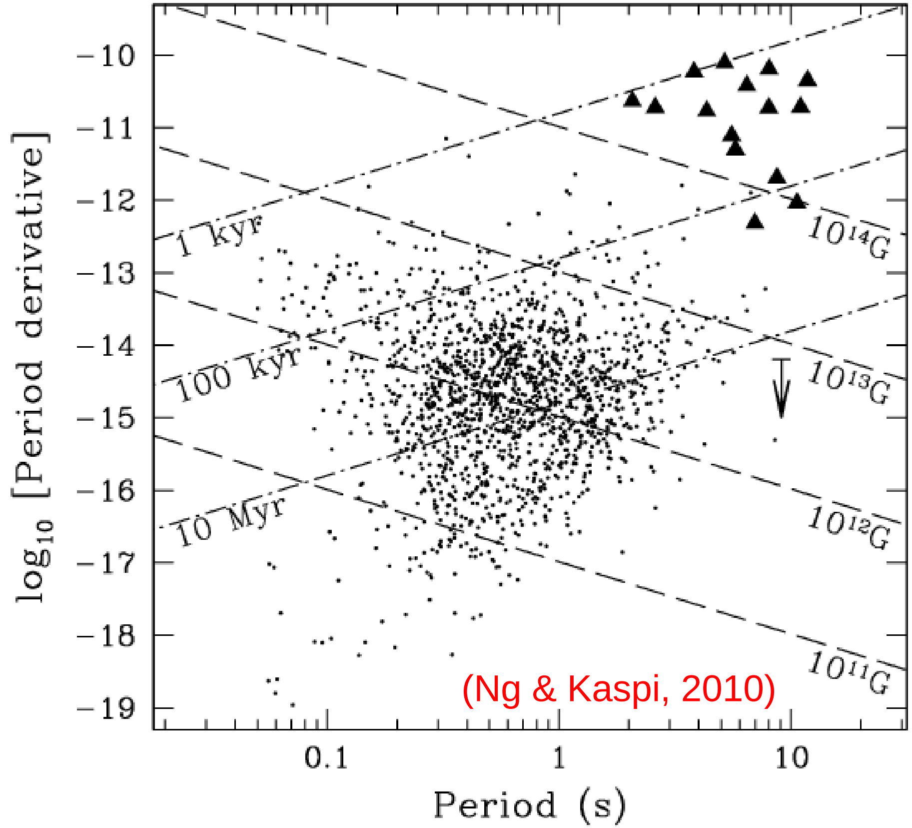

(Ng & Kaspi, 2010)

$$f = \begin{cases} \frac{2}{3}\sin^2\theta_B & \text{in vacuum} \\ 1 + \sin^2\theta_B & \text{force free} \end{cases}$$

$$L_{\rm sd} = f\frac{B_s^2 R_{NS}^6 \Omega^4}{c^3} \rightarrow B_s = 3.2\times 10^{19}\sqrt{P\dot{P}}\ \mathrm{G} > B_Q = \frac{m_e^2 c^3}{e\hbar} = 4.4\times 10^{13}\ \mathrm{G}$$

- High quiescent X-ray luminosities: $L_X \sim 10^{33} - 10^{36}\ \mathrm{erg\ s^{-1}} > L_{\rm sd}$

Magnetars: differences from “normal” pulsars

- Magnetars (especially SGRs) show diverse bursting activity, from small bursts to giant flares

- Giant flares are rare (only 3 observed so far) & extremely luminous bursts:

$$L_{\rm pk} \sim 10^{44} - 10^{47} \ {\rm erg \ s^{-1}}$$

(Woods & Thompson 2004)

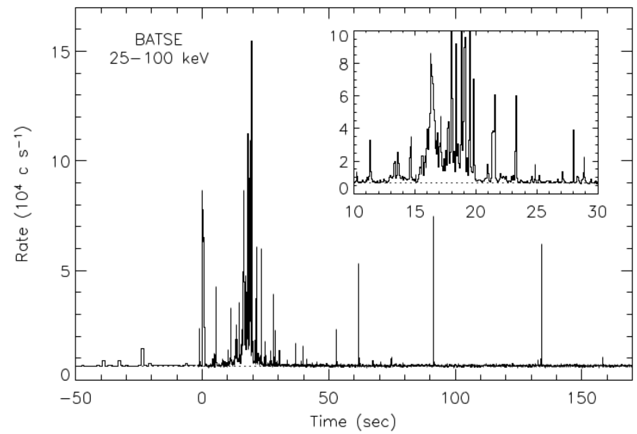

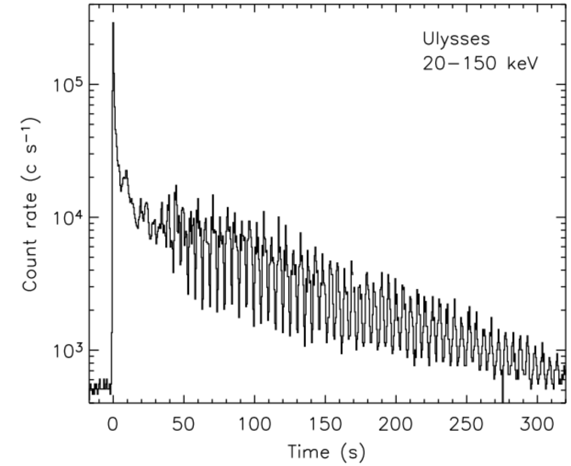

- These observations led to the Thompson & Duncan (1993, 1995, 1996, 2000) magnetar model, which posits that:
  - Magnetar bursts and quiescent emission is powered by the decay of the strong internal magnetic field $B_{\rm int} \gtrsim 10^{15}$ G
  - Short bursts are related to stressing of the crust by the unwinding internal toroidal field.
  - Giant flares are produced by shearing and reconnection of the strong external magnetic field.
  - High magnetic fields in magnetars result from field amplification by a dynamo mechanism when $P_0 \lesssim 3$ ms

(TD96)

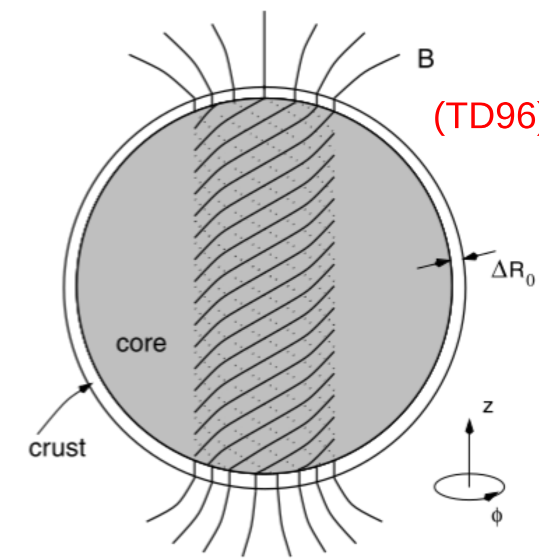

Pulsar Wind Nebulae (PWNe)

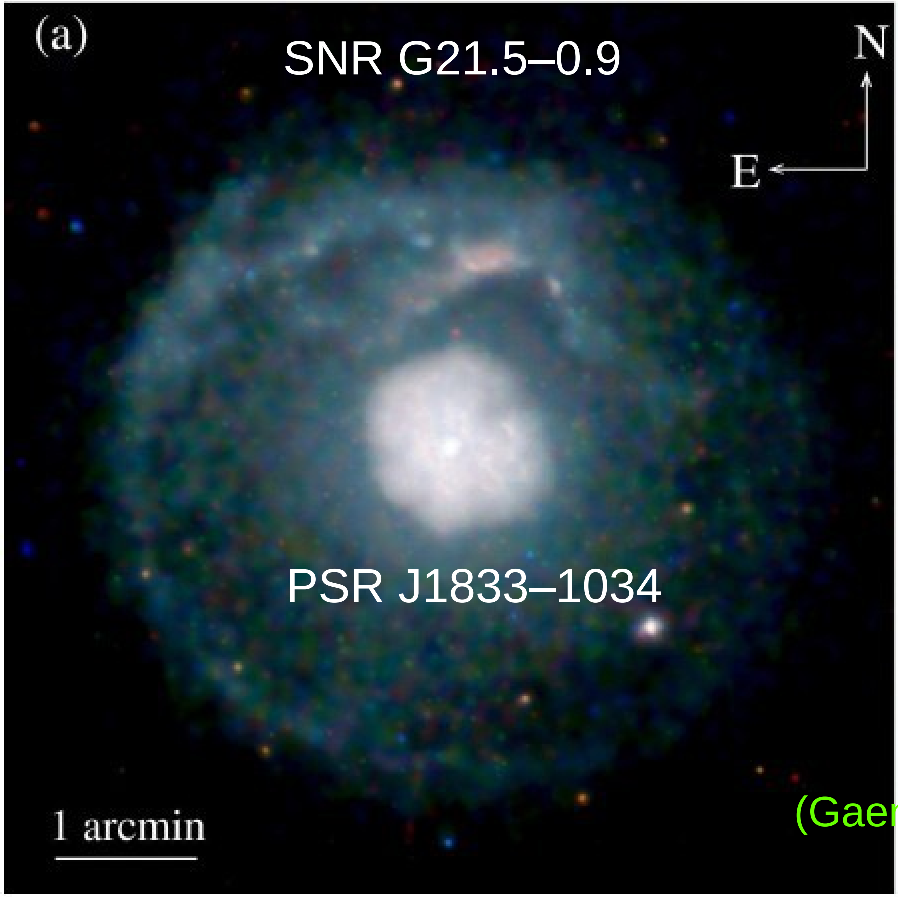

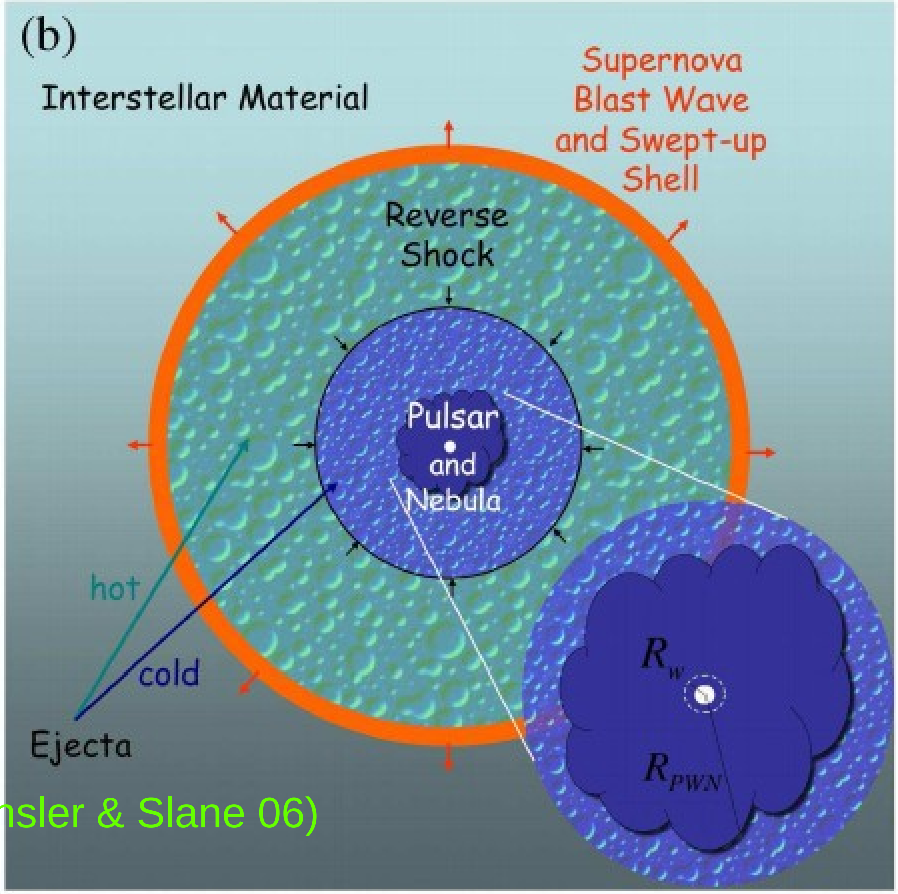

(Gaensler & Slane 06)

The Crab

- Cold ultra-relativistic MHD wind is launched from the pulsar, powered by $\dot{E}_{rot}$
- This wind is decelerated & heated at the termination shock radius, R_{TS}, where its ram-pressure equals the pressure in the hot nebula that it inflates
- The hot, high-pressure nebula is bounded by the SNR & performs work on it

$$L_{\rm sd} = 4\pi R^2 c P \qquad P = \frac{e}{3} = \frac{E_{\rm neb}}{4\pi R_{\rm neb}^3} \qquad R_{TS} = \sqrt{\frac{R_{\rm neb}^3 L_{\rm sd}}{c E_{\rm neb}}}$$

The first-ever magnetar wind nebula

- NuSTAR (3 – 30keV)
- XMM (0.5 – 10 keV)
- Fermi GeV
  H.E.S.S TeV
- Radio

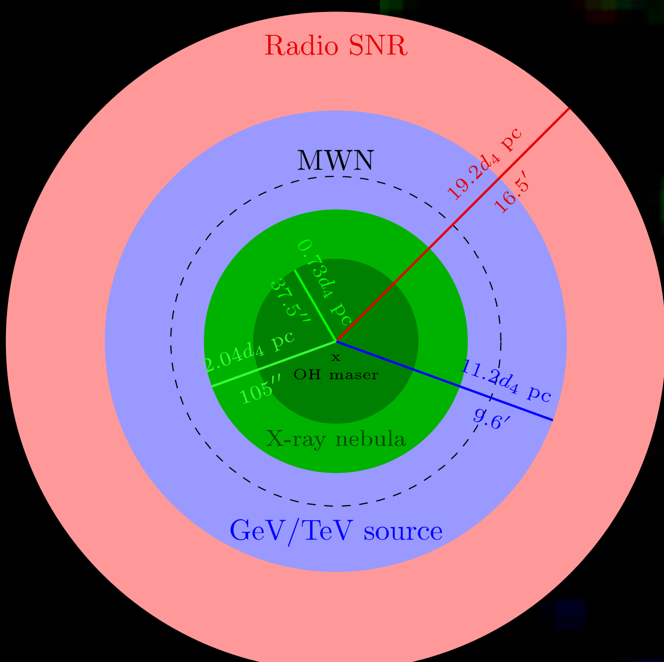

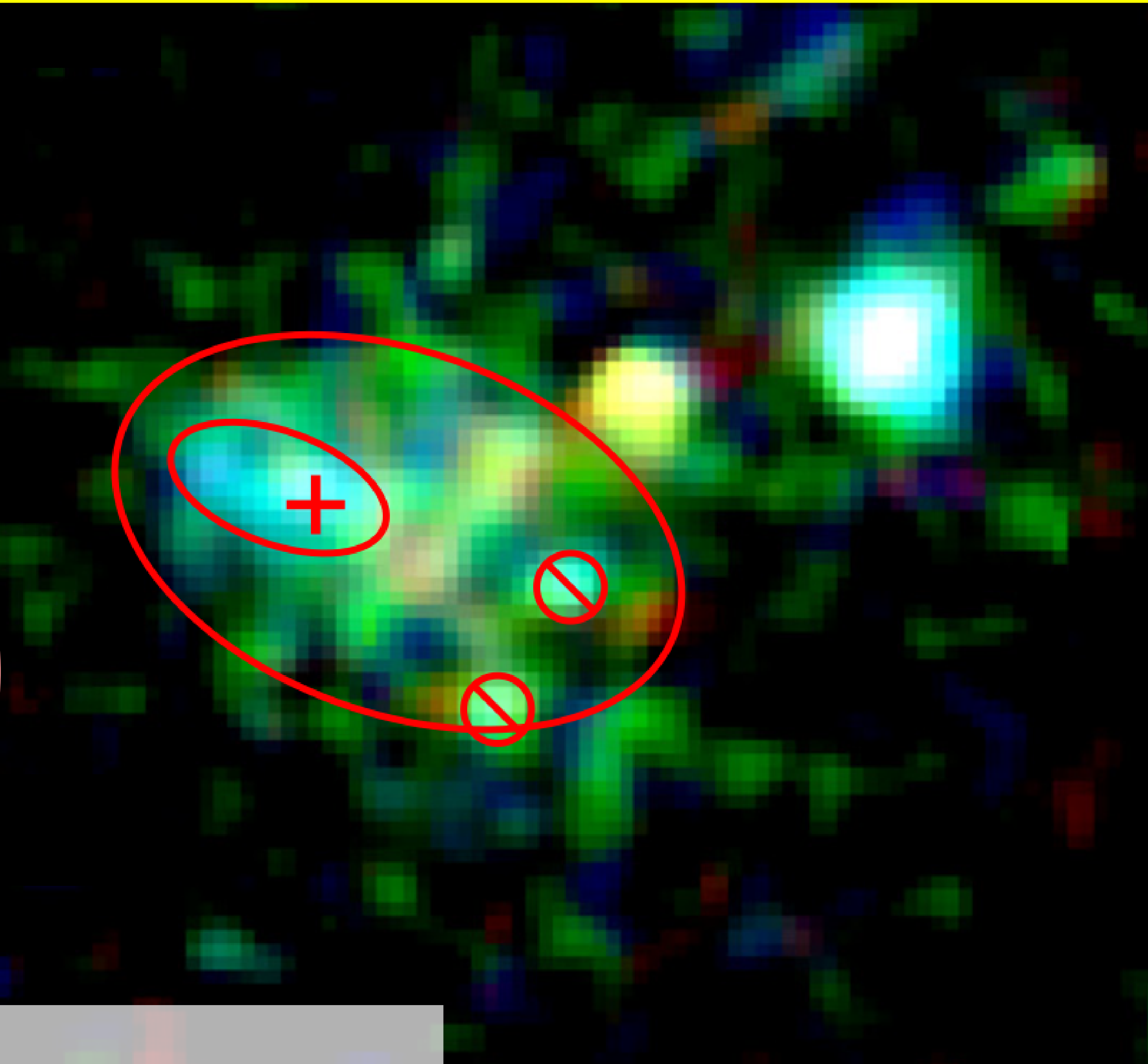

Swift J1834.9-0846

$P = 2.48$ s

$\dot{P} = 7.96 \times 10^{-12}$ s s^{-1}

$\tau_c = 4.9$ kyr $\quad (n = 3)$

$t = \tau_c - 10^5$ yr

$B_s = 10^{14}$ G

$L_{\rm sd} = 2 \times 10^{34}$ erg s^{-1}

(Younes et al. 2016)

XMM-Newton observations

(2-3 keV, 3-4.5 keV, 4.5-10 keV)

Association with SNR W41 & Efficiency of MWN's X-ray emission

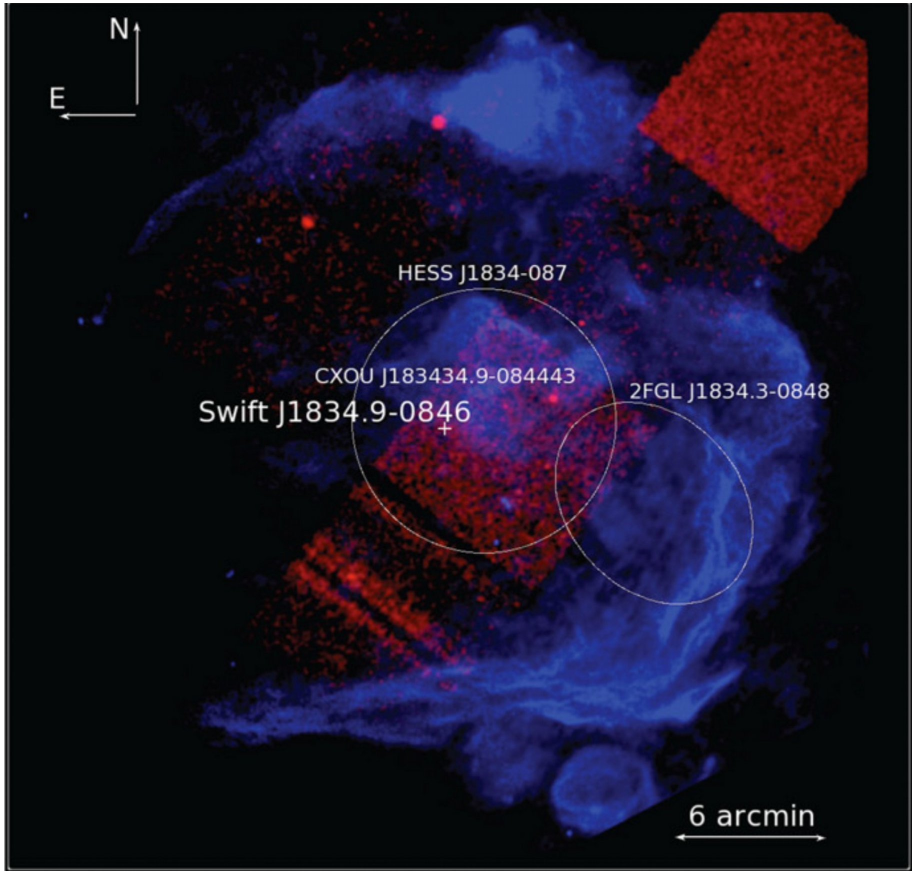

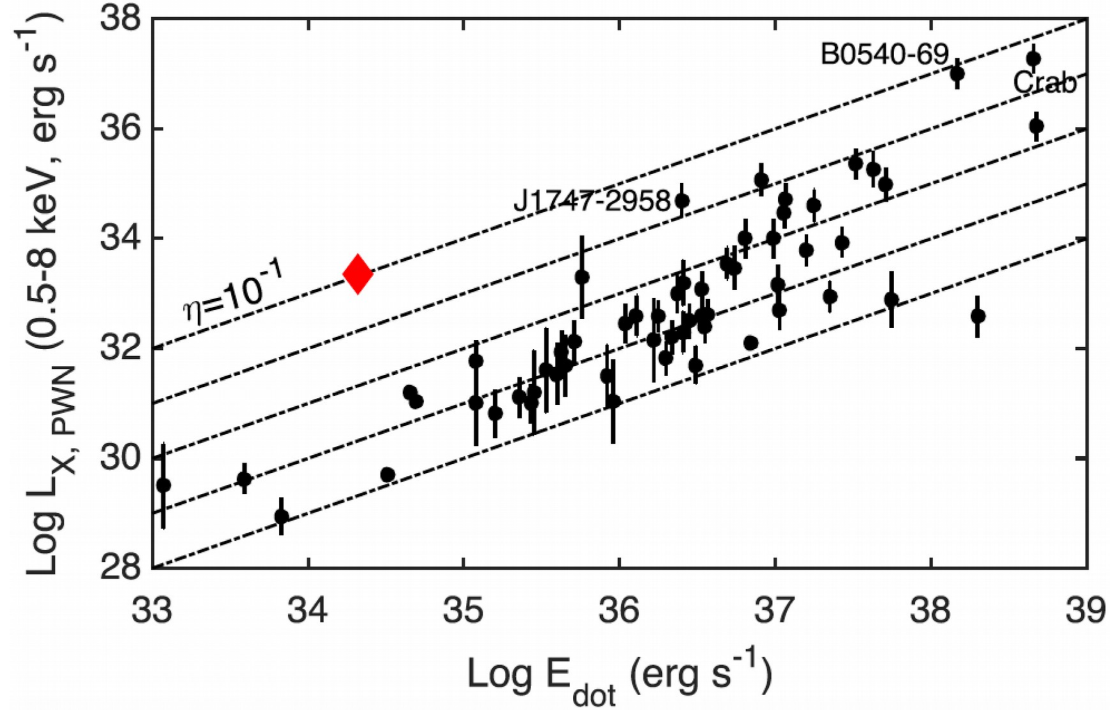

$$R_{\rm SGR} \lesssim (0.05 - 0.1) R_{\rm SNR}$$

$$\Downarrow$$

$$v_{\perp,\rm SGR} \lesssim (30 - 60) \left(\frac{t_{\rm SNR}}{10^{4.5}\,\rm yr} \right) d_4 \ \rm km/s$$

$$d_4 \equiv d/4\,\rm kpc$$

Total emitted power (0.5 – 30 keV)

$$L_{\rm x,tot} = 2.74 \times 10^{33} d_4^2 \ \rm erg/s$$

The spin-down power

$$L_{\rm sd} = 2.05 \times 10^{34} \ \rm erg/s$$

X-ray efficiency of MWN

$$\eta_X = \frac{L_{\rm X,tot}}{L_{\rm sd}} = 0.13 d_4^2$$

Association with SNR W41 & Efficiency of MWN's X-ray emission

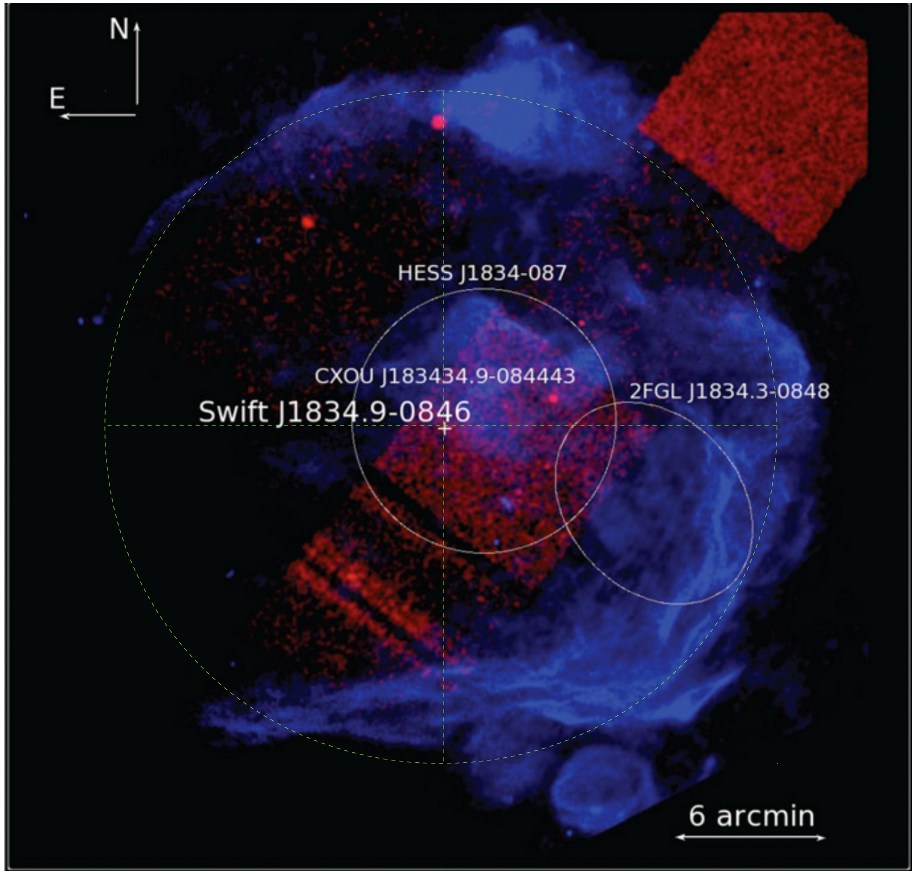

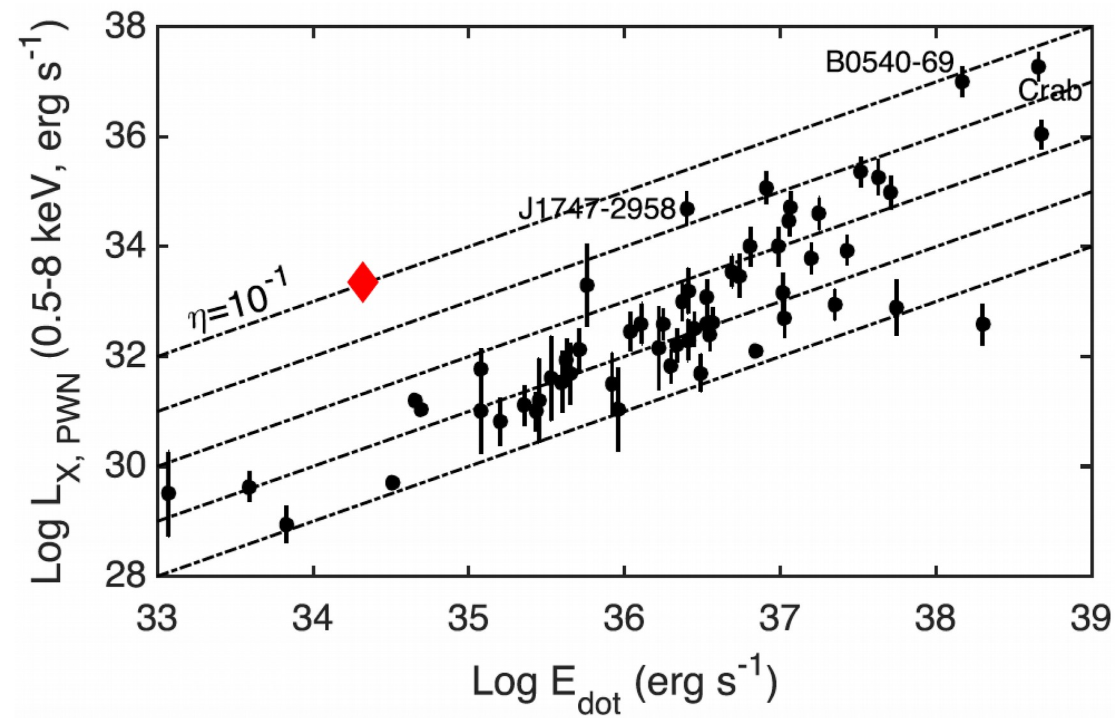

$$R_{\rm SGR} \lesssim (0.05 - 0.1) R_{\rm SNR}$$

$$\Downarrow$$

$$v_{\perp,{\rm SGR}} \lesssim (30 - 60) \left(\frac{t_{\rm SNR}}{10^{4.5}\,{\rm yr}} \right) d_4 \ {\rm km/s}$$

$$d_4 \equiv d/4\,{\rm kpc}$$

Total emitted power (0.5 – 30 keV)

$$L_{\rm x,tot} = 2.74 \times 10^{33} d_4^2 \ {\rm erg/s}$$

The spin-down power

$$L_{\rm sd} = 2.05 \times 10^{34} \ {\rm erg/s}$$

X-ray efficiency of MWN

$$\eta_X = \frac{L_{\rm X,tot}}{L_{\rm sd}} = 0.13 d_4^2$$

The Detectability of Magnetar Wind Nebulae

- Is Swift J1846.9–0846 really unique (J1935)? What helps make a MWN detectable?
- It is currently ~1-2 MWNe around ~30 known magnetars (small number statistics)
- What makes the difference? Intrinsic vs. External properties:
- Current spin-down power L_{sd}
- Initial spin period P_0 & rotational energy E_0
- Initial surface dipole field B_0
- Pair multiplicity & wind Lorentz factor
- Natal kick velocity

Small kick velocity: magnetar remains inside its SNR, which confines a MWN (traps the outflows & results in a relatively bright, easier to detect emission)

$$\mathrm{offset} \lesssim (0.05-0.1)\mathrm{R_{SNR}} \Longrightarrow \mathrm{v_{\perp,SGR}} \lesssim (30-60)\mathrm{d_4(t_{SNR}/10^{4.5}\ yr)^{-1}\ km\ s^{-1}}.$$

Large kick velocity: magnetar exits its SNR & forms a bow-shock containing much less energy (most of the outflow escapes, leading to weaker, harder to detect emission)

$$\mathrm{SGR\ 1806{-}20:\ v_{\perp,SGR} \approx 580 d_{15}\ km\ s^{-1}}\ ,\quad \mathrm{SGR\ 1900{+}14\ v_{\perp,SGR} = 130 \pm 30\ km\ s^{-1}}$$

$$\mathrm{SGR\ 0501{+}4516:\ v_{\perp,SGR} \sim 3000\ km\ s^{-1}}\ ,\quad \mathrm{SGR\ 0526{-}66\ v_{\perp,SGR} \approx 1100\ km\ s^{-1}}$$

- **External density (SNR & MWN evolution) + composition (bow shock X-ray efficiency)**

Dynamics of the MWN + SNR

- The SN ejecta initially expands ballistically:

$$\rho_{\rm ej}(r,t) = A t^{-3} \,, \qquad r < v_t t$$

$$\rho_{\rm ej}(r,t) = A v_t^s r^{-s} t^{s-3} \,, \qquad r > v_t t$$

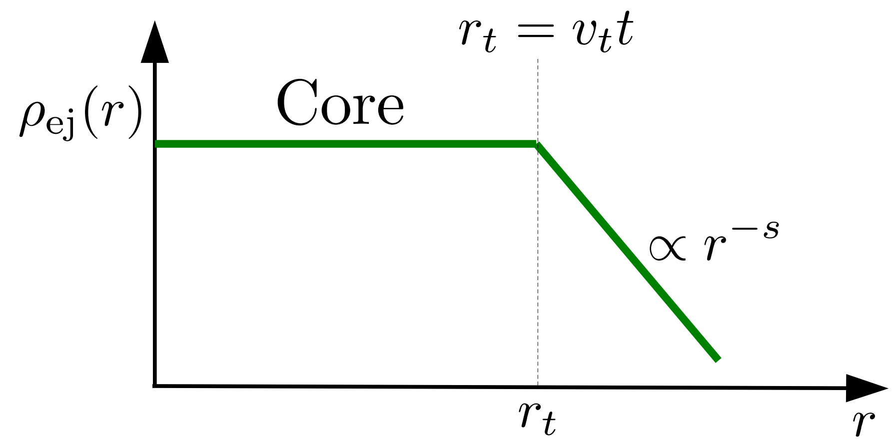

$$m = (n+1)/(n-1)$$

Energy injection by the magnetar: $L_{\rm sd} = L_0 \left(1 + \frac{t}{t_0}\right)^{-m} \approx L_0 \times \begin{cases} 1 & t < t_0 \\ (t/t_0)^{-m} & t > t_0 \end{cases}$

Core crossing time by MWN: t_c

$$t_0 < t_c : \quad P_0 > 4.1 \left[\frac{n-1}{2} E_{\rm SN,51}\right]^{-1/2} \,{\rm ms} \qquad E_0 < 1.2 \times 10^{51} \left(\frac{n-1}{2}\right) E_{\rm SN,51} \,{\rm erg}$$

$$t_{\rm ST} = 519 M_3^{5/6} E_{\rm tot,51}^{-1/2} n_0^{-1/3} \,{\rm yr}$$
$$= 116 M_3^{5/6} E_{\rm tot,52.3}^{-1/2} n_0^{-1/3} \,{\rm yr}$$

$$R_{\rm ST} = 3.07 M_3^{1/3} n_0^{-1/3} \,{\rm pc}$$

$$E_{\rm tot} = E_0 + E_{\rm SN}$$

$$E_0 = \frac{n-1}{2} L_0 t_0 = \frac{1}{2} I \Omega_0^2 \simeq 2 \times 10^{52} P_{\rm 0,ms}^{-2} \,{\rm erg}$$

$$t_0 = 1.3 \times 10^5 \frac{2}{n-1} f^{-1} B_{14}^{-2} P_{\rm 0,ms}^2 \,{\rm s}$$

Evolution of MWN & SNR Radii

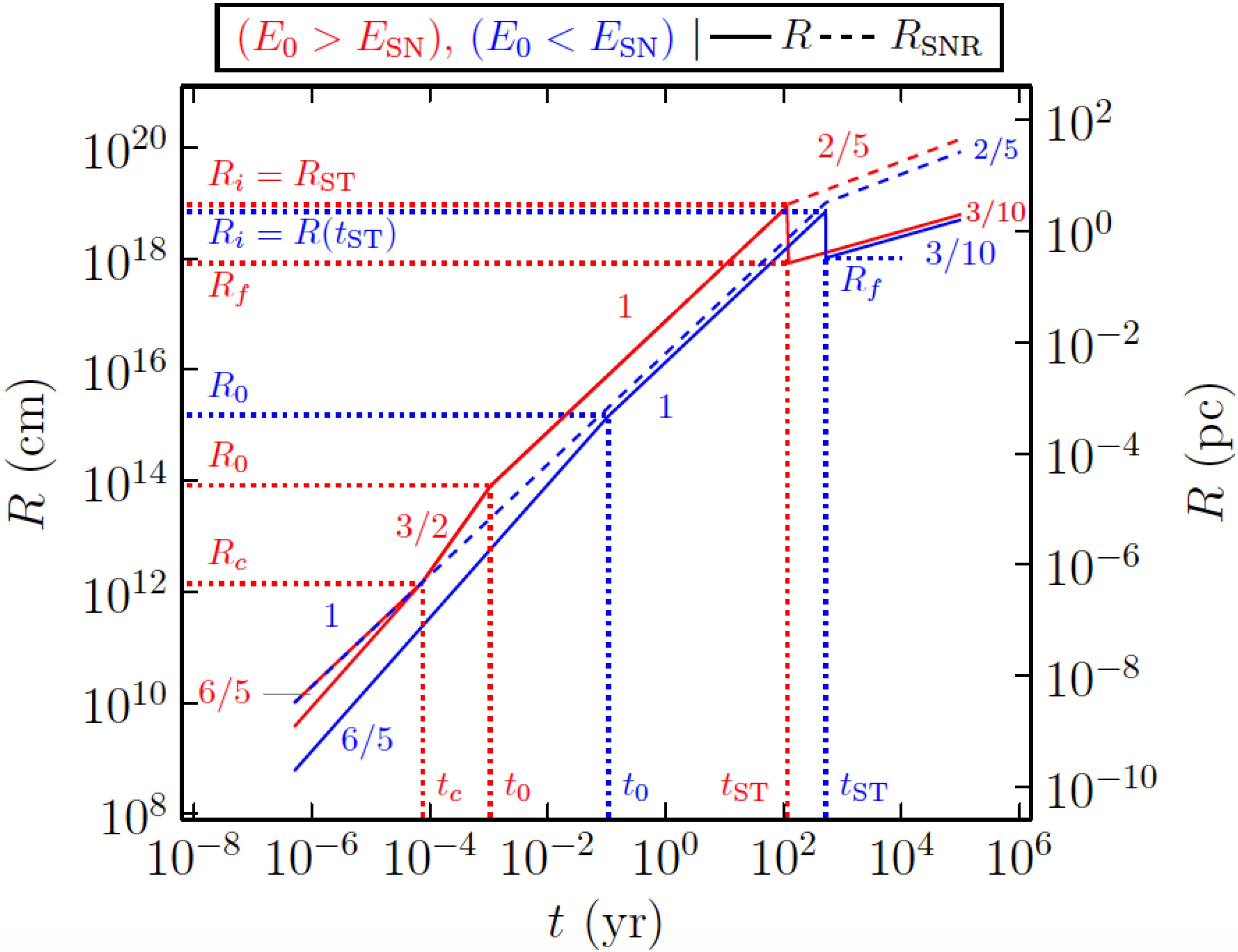

Evolution of MWN & SNR Energies

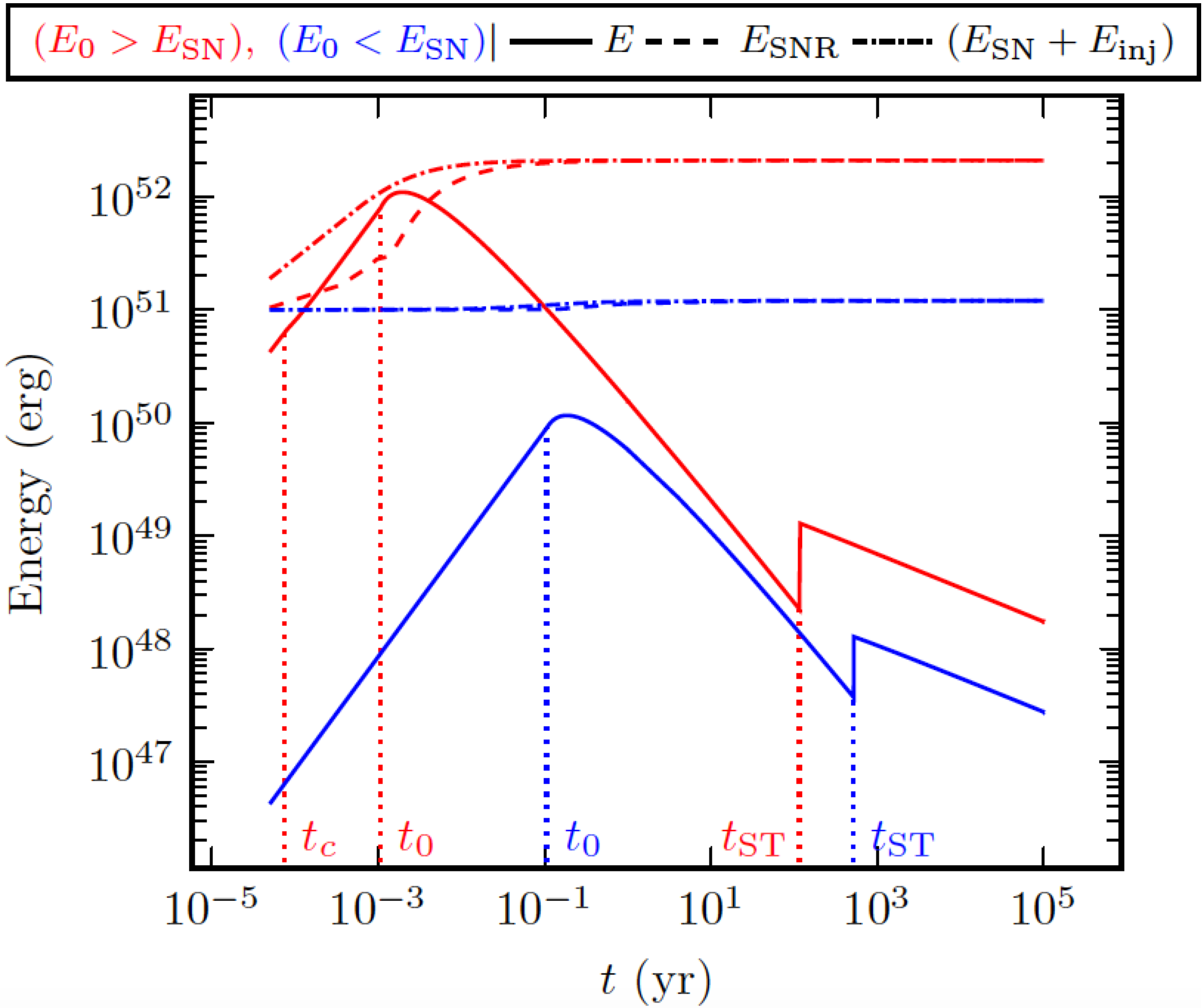

The MWN internal flow structure

- In contrast with the usual ideal MHD assumption (Kennel & Coroniti 84’) motivated by recent 3D RMHD simulations we assume a non-ideal low-σ flow (MHD → HD; BM76)

- In the inner-nebula there is a quasi-steady flow:

$$\frac{\partial}{\partial t}(\tilde{n}\gamma) + \frac{c}{r^2}\frac{\partial}{\partial r}(r^2\tilde{n}\gamma\beta) = 0\ , \quad \frac{d}{dt}P\tilde{n}^{4/3} = 0\ , \quad \frac{d}{dt}(P\gamma^4) = \gamma^2\frac{\partial P}{\partial t} \implies \beta(r) \approx \frac{1}{3}\left(\frac{r}{R_{\rm TS}}\right)^{-2}$$

- Velocity continuity with v_{SNR} at the outer radius R & equating the wind ram pressure to the nebula’s thermal pressure at R_{TS} implies a uniformly expanding outer region

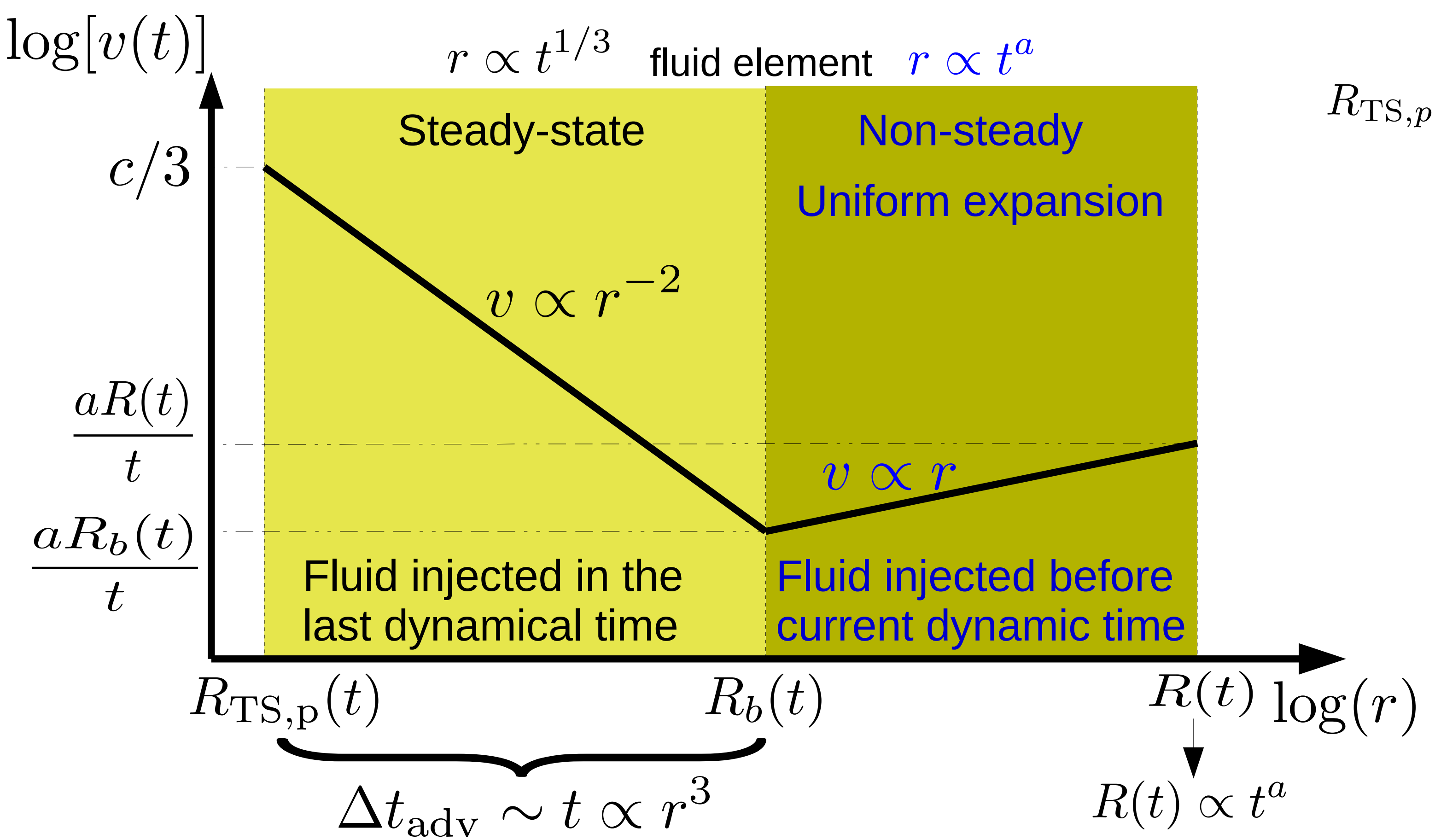

$$R_{{\rm TS},p}(t) = \sqrt{\frac{R(t)^3 L_{\rm sd}(t)}{cE(t)}} \propto t^{(4a-m)/2}$$

$$\left(\frac{R_b(t)}{R(t)}\right)^3 = \frac{tL_{\rm sd}(t)}{3aE(t)}$$

$$a = \frac{3}{2(5-k)} \to 0.3 \ \ (t > t_{\rm ST})$$

Observed Size & Spectral Softening: Roles of Diffusion & Cooling

Synchrotron **cooling time** of X-ray emitting electrons (at $2E_2$ keV) is << system's age ⇒ quasi-steady state:

$$t_{\rm syn} = \frac{6\pi m_e c}{\sigma_T B^2 \gamma_e} \simeq 1.02 B_{15\mu{\rm G}}^{-3/2} E_2^{-1/2}\ {\rm kyr}\ .$$

- Diffusion dominates over advection in whole MWN

$$r_{c,{\rm dif}} \approx \sqrt{2\lambda_{\rm def} c t_{\rm syn}(\gamma_e)} \approx 1.57\, B_{15\mu{\rm G}}^{-3/2} \zeta^{1/2}\ {\rm pc}$$

$$\zeta \equiv \lambda_{\rm def}/R_L \gtrsim 1\ (\zeta = 1 \text{ corresponds to Bohm diffusion})$$

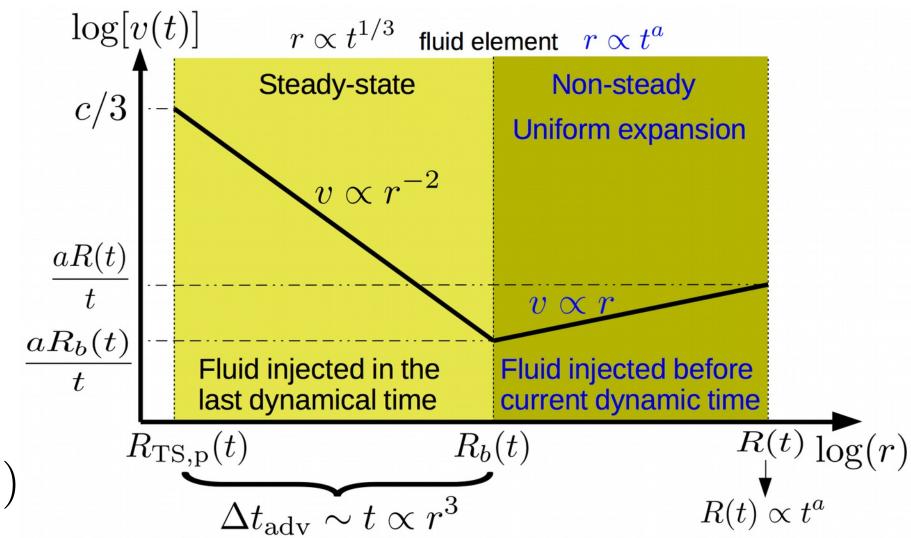

- Resulting cooling length ~ observed nebula size R_X ⇒ may also explain the spectral softening (from $\Gamma_x = 1.41 \pm 0.12$ in the inner nebula to $\Gamma_x = 2.5 \pm 0.2$ in the outer nebula)

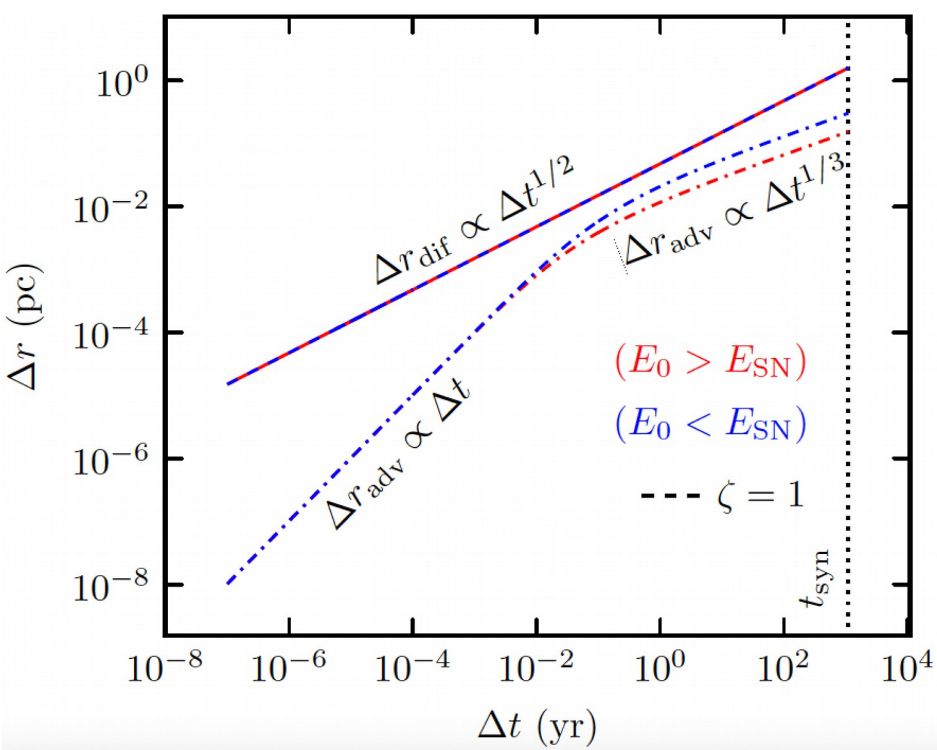

$B_{15\mu{\rm G}} = 1$

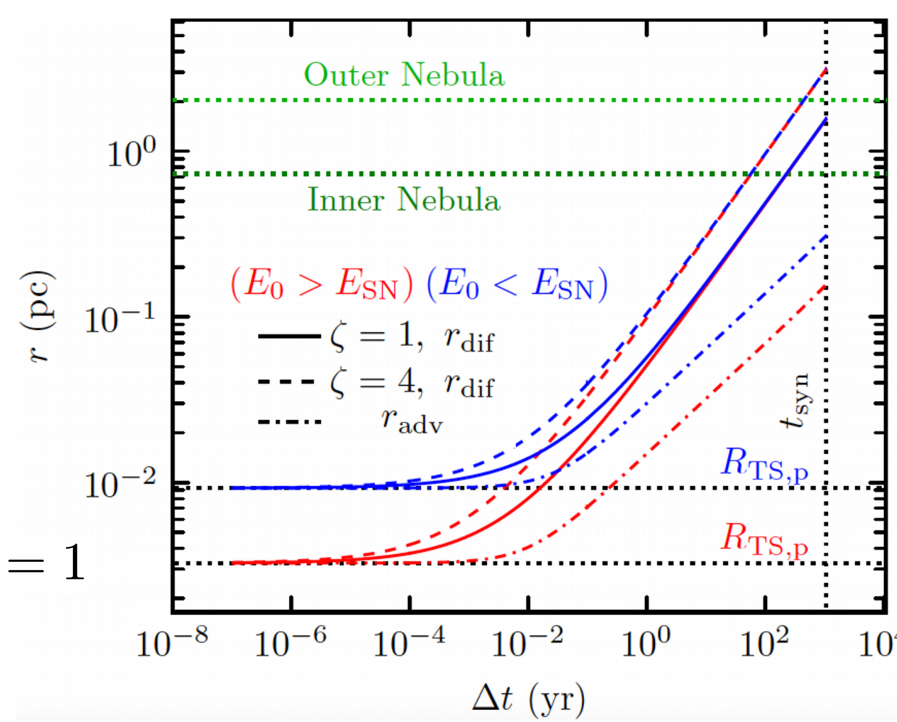

The Synchrotron X-Ray Nebula around Swift 1834.9–0846

- Magnetic field in the X-ray emitting region is:

$$B = \left(\frac{L_X \sigma_e}{\mathcal{A} V} \frac{\Gamma - 2}{\Gamma - 1.5} \frac{\nu_1^{1.5-\Gamma} - \nu_2^{1.5-\Gamma}}{\nu_m^{2-\Gamma} - \nu_M^{2-\Gamma}} \right)^{2/7}$$

$$\simeq \begin{cases} 4.0 \xi \sigma_e^{2/7} d_4^{-2/7}\ \mu\text{G} & \text{(whole nebula)}, \\ 5.0 \xi_{\text{in}} \sigma_e^{2/7} d_4^{-2/7}\ \mu\text{G} & \text{(inner nebula)}. \end{cases}$$

Observation: XMM (0.5 – 10 keV)

$L_x = 2.5 \times 10^{33} d_4^2$ erg s^{-1} $\quad \Gamma = 2.2 \pm 0.2$

$\Gamma_{\text{in}} = 1.3 \pm 0.3 \quad \Gamma_{\text{out}} = 2.5 \pm 0.2$

NuSTAR detected inner nebula up to 30 keV

XMM + NuSTAR (0.5–30 keV) joint fit results:

$L_{\text{in}} = 5.0 \times 10^{32} d_4^2$ erg s^{-1} $\quad \Gamma_{\text{in}} = 1.41 \pm 0.12$

Assuming:

- Power-law electron distribution: $\frac{dN_e}{d\gamma_e} \propto \gamma_e^{-p} \quad \gamma_1 < \gamma_e < \gamma_2$
- Electrons emitting in observed range: $\gamma_1 < \gamma_m < \gamma_e < \gamma_M < \gamma_2$
- Magnetization: $\sigma = \frac{B^2}{4\pi w} = \frac{3}{2}\frac{B^2}{8\pi e} = \frac{3}{2}\frac{E_B}{E_m} = \frac{3}{2}\sigma_e \epsilon_e$
- Emission volume: $V = \frac{4}{3}\pi R_x^3$

$\sigma_e \equiv E_B / E_e$

X-ray efficiency of MWN

$$\eta_X = \frac{L_{\text{X,tot}}}{L_{\text{sd}}} = 0.13 d_4^2$$

$E_e = \epsilon_e E_m$

(E_m = total energy in matter in the emission region)

$$\xi^{7/2}(\nu_1, \nu_2) = \left(\frac{\nu_2^{1.5-\Gamma} - \nu_1^{1.5-\Gamma}}{\nu_M^{1.5-\Gamma} - \nu_m^{1.5-\Gamma}} \right)$$

= ratio of energy in all electrons to that in those radiating in the observed frequency range

Constraints From Maximum Electron Lorentz Factor

(De Jager & Harding 92)

Maximum injected L.F.: $\gamma_{\max} = \frac{e R_{NS}^3 \Omega^2 B_s}{m_e c^4} = \frac{e}{m_e c^2}\sqrt{\frac{L_{sd}}{fc}} = \frac{4.9 \cdot 10^8}{\sqrt{f}}$
(corresponding to acc. ir. the potential difference across the open field lines)

$$\gamma_{\max} > \gamma_M$$

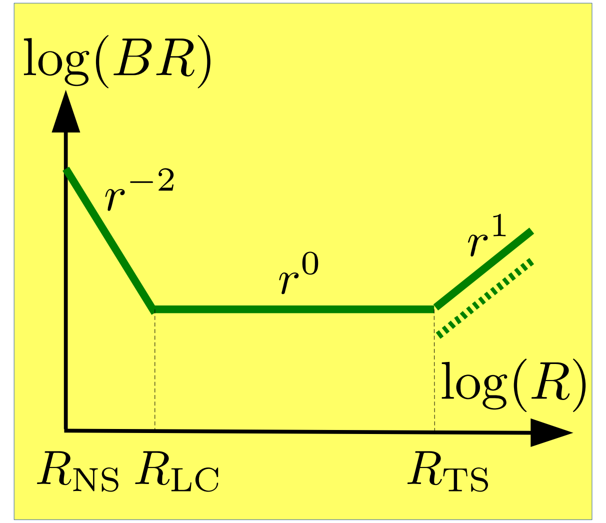

Max. obs. energy:
$E_X = 30 E_{M,30}$ keV

$$B > B_{\min} \equiv \frac{m_e^3 c^6 f E_X}{\hbar e^3 L_{sd}} \simeq 11.0 f E_{M,30}\ \mu\text{G}$$

which further yields

$$\sigma_e > 0.043\, d_4 \left(\frac{f E_{M,30}}{\xi_7}\right)^{\frac{7}{2}},$$

$$\sigma_{e,\text{in}} > 0.055\, d_4 \left(\frac{f E_{M,30}}{\xi_{\text{in}}/5}\right)^{\frac{7}{2}}.$$

$$\xi > 16.1\, f E_{M,30} \left(\frac{\epsilon_e d_4}{\sigma_{-2.5}}\right)^{\frac{2}{7}},$$

$$\xi_{\text{in}} > 12.7\, f E_{M,30} \left(\frac{\epsilon_e d_4}{\sigma_{\text{in},-2.5}}\right)^{\frac{2}{7}},$$

Synchrotron **cooling time** of X-ray emitting electrons: (at $2E_2$ keV) is << system's age → quasi-steady state

$$t_{\text{syn}} = \frac{6\pi m_e c}{\sigma_T B^2 \gamma_e} \simeq 1.02 B_{15\mu G}^{-3/2} E_2^{-1/2}\ \text{kyr}\ .$$

Electron energy balance: $\langle \dot{E} \rangle = g L_{sd} = \frac{(1+\sigma)}{\epsilon_e \epsilon_X} L_{X,\text{tot}}$

In terms of the observed X-ray efficiency:

$$g = \frac{L_{X,\text{tot}}}{L_{sd}} \frac{(1+\sigma)\xi^{7/2}}{\epsilon_e} = \frac{\eta_X (1+\sigma)\xi^{7/2}}{\epsilon_e}$$

Estimate of ξ_{in} from the inner nebula yields:

$$\frac{g\sigma}{1+\sigma} > 3.07 d_4^3 E_{M,30}^{7/2} f^{7/2}$$

$(1+\sigma)^{-1}$ = fraction of the total energy injected into the nebula going to particles (the rest goes into the B-field)

ϵ_e = fraction of that going into power-law energy dist. of electrons

$\epsilon_X = \xi^{-7/2}$ = fraction of that going into electrons radiating observed X-rays

What powers the MWN? Rotational energy is not enough

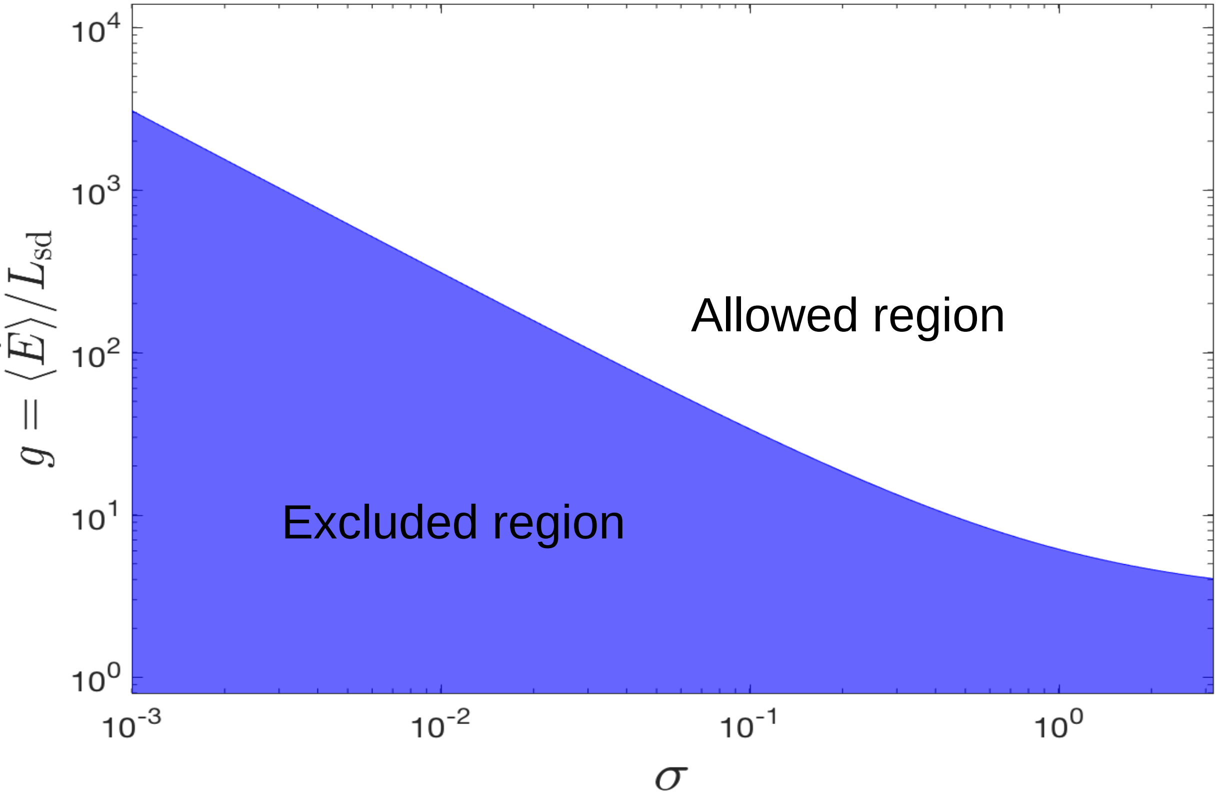

- **$\dot{E}_{rot}$ is not enough to power the MWN!!!**

Lower X-ray efficiency: $\langle \dot{E} \rangle = g L_{sd} \Longrightarrow \eta_{X,\mathrm{true}} = \frac{L_{X,\mathrm{tot}}}{\langle \dot{E} \rangle} = \frac{\eta_X}{g} = \frac{0.0026 d_4^2}{g_{50}} < 0.042 \frac{\sigma}{1+\sigma} d_4^{-1} E_{M,30}^{-\frac{7}{2}} f^{-\frac{7}{2}}$

Electron energy balance: $\langle \dot{E} \rangle = g L_{sd} = \frac{(1+\sigma)}{\epsilon_e \epsilon_X} L_{X,\mathrm{tot}}$

In terms of the observed X-ray efficiency:

$$g = \frac{L_{X,\mathrm{tot}}}{L_{sd}} \frac{(1+\sigma)\xi^{7/2}}{\epsilon_e} = \frac{\eta_X (1+\sigma)\xi^{7/2}}{\epsilon_e}$$

Estimate of ξ_{in} from the inner nebula yields: $\frac{g\sigma}{1+\sigma} > 3.07 d_4^3 E_{M,30}^{7/2} f^{7/2}$

$(1+\sigma)^{-1}$ = fraction of the total energy injected into the nebula going to particles (the rest goes into the B-field)

ϵ_e = fraction of that going into power-law energy dist. of electrons

$\epsilon_X = \xi^{-7/2}$ = fraction of that going into electrons radiating observed X-rays

Can the decaying dipole field power the MWN?

- A potential energy source is the decay of the super-strong magnetar dipole magnetic field

Dipole Field Decay:

$$B_s(t) = B_0 \left(1 + \frac{t}{t_B}\right)^{-1/\alpha} \equiv B_0 \tau^{-1/\alpha}$$

$$\dot{E}_{\rm dip} = \frac{d}{dt}\left(\frac{B_s^2 R_{\rm NS}^3}{6}\right) = -\frac{2}{\alpha}\frac{E_{B,\rm dip}(t)}{t_B \tau}$$

Since t_B is not well constrained, we find which decay timescale maximizes the the power

$$|\dot{E}_{B,\rm dip}|_{\rm max} = \frac{2}{2+\alpha}\frac{E_{B,\rm dip}(t)}{t}$$

$$t_B = 2t/\alpha \qquad \tau_{\rm max} = 1 + \alpha/2$$

Comparison of this power with that required to power the nebula gives

$$\frac{|\dot{E}_{B,\rm dip}|_{\rm max}}{g L_{\rm sd}} = 1.25 \times 10^{-3} g_{50}^{-1} f^{-1} t_{4.5}^{-1}$$

$$g = 50 g_{50} \quad t_{\rm SNR} = 10^{4.5} t_{4.5} \text{ yr} \quad \alpha = 3/2$$

(motivated by Dall'Osso, JG & Piran 2012)

Decay of dipole field alone cannot supply the requisite power $\langle \dot{E} \rangle = g L_{\rm sd}$

Decay of the stronger internal magnetic field B_{int} is needed

Internal Field Decay: We demand that the maximum field decay power slightly exceeds the required power due to inefficiencies in power transfer to particles

$$|\dot{E}_{B,\mathrm{int}}|_{\max} = \frac{2}{2+\alpha}\frac{E_{B,\mathrm{int}}(t)}{t} \geq g L_{\mathrm{sd}} \longrightarrow B_{\mathrm{int}}(t) \geq 3.3\times 10^{15} g_{50}^{1/2} t_{4.5}^{1/2}\ \mathrm{G}$$

- Stability requires that B_{int}/B_{dip} cannot be too large; Simulations find (Braithwaite 2009):

  (I) the configuration is stable when both poloidal & toroidal components exist

  (II) the ratio of the two components is constrained

$$\mathcal{A}E_{\mathrm{B,int}}/E_G \simeq 10^{-3} \lesssim E_{\mathrm{B,dip}}/E_{\mathrm{B,int}} \lesssim 0.8$$

$$E_G \simeq 3\times 10^{53}\ \mathrm{erg}$$

(Gravitational binding energy)

$$\mathcal{A} \sim 10^3 \quad \text{(for NSs)}$$

- The lower limit yields the maximum internal field

$$B_{\mathrm{int}} \lesssim B_{\mathrm{int,max}} = \left(\frac{6E_G B_{\mathrm{dip},0}^2}{\mathcal{A}R_{\mathrm{NS}}^3}\right)^{1/4} = 6.6\times 10^{15} B_{\mathrm{dip},0,15}^{1/2}\ \mathrm{G}$$

$$\longrightarrow g \leq g_{\max} = \frac{2}{2+\alpha}\frac{R_{\mathrm{NS}}^3 B_{\mathrm{int,max}}^2}{6L_{\mathrm{sd}}t}$$

- Consistent with the results of Dall'Osso et al. (2012), which favor a young age $t \lesssim 10^{4.5}$ yr

$$B_{\mathrm{int},0} \sim (1-3)\times 10^{16}\ \mathrm{G}\ , \quad \alpha_{\mathrm{int}} \sim 1-1.5\ , \quad t_{B_{\mathrm{int}}} \sim 7-10\,\mathrm{kyr}$$

$g - \sigma$ plane

Assuming the fiducial age: $t_{\rm SNR} = 10^{4.5}$ yr

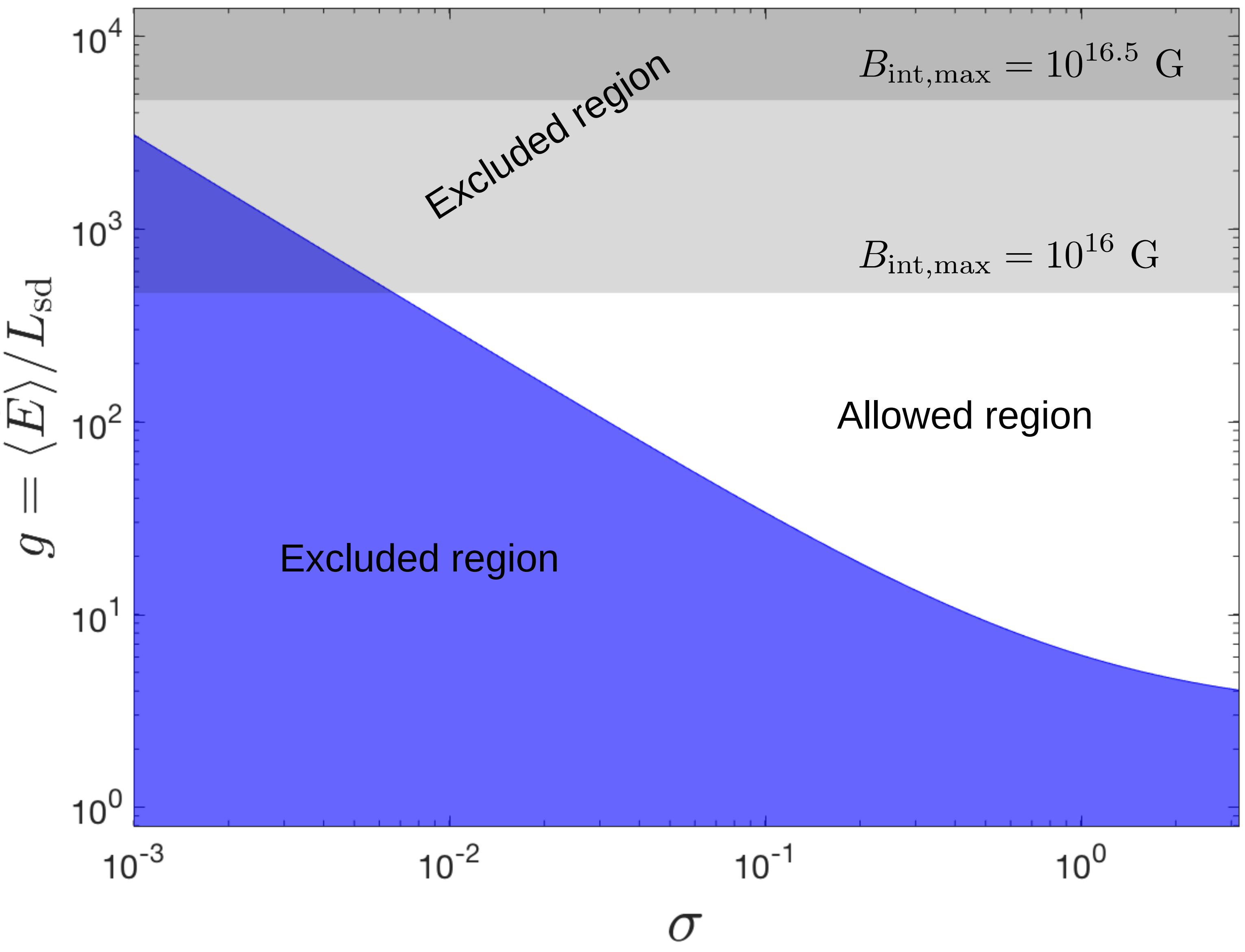

Energy injection through bursts & flares

- A natural mechanism for additional energy injection into the MWN is through bursts and giant flares, but how many bursts are required?

SGR 1806-20

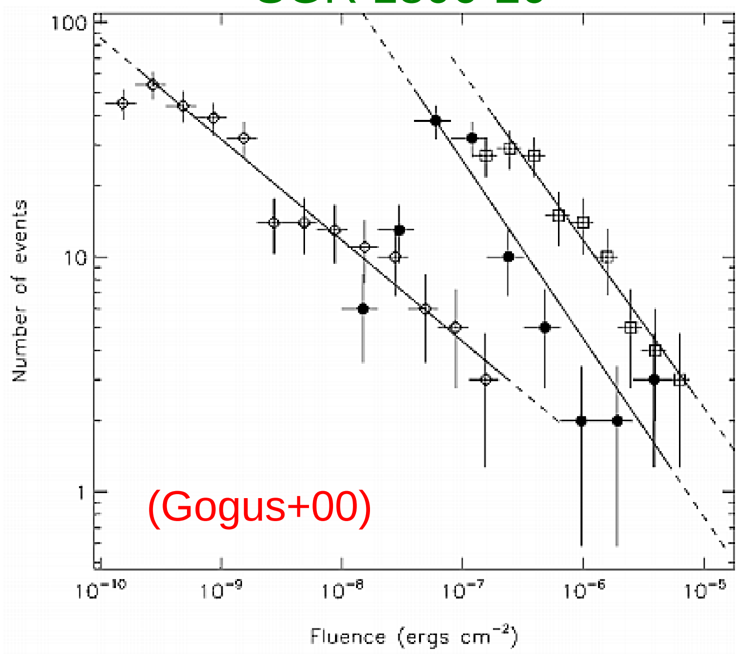

SGR 1900+14

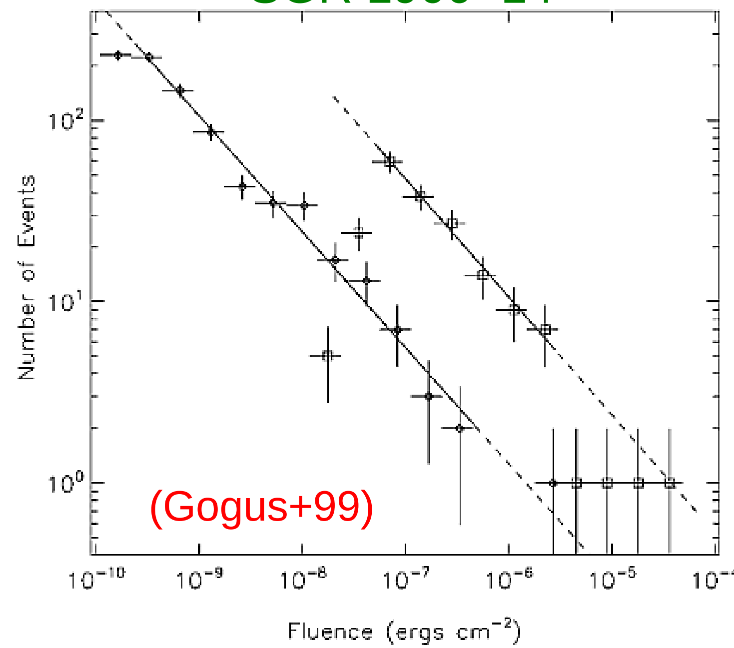

- Energy distribution of magnetar bursts appear to follow a power-law: $E^2 \frac{dN}{dE} \propto E^{-s+2}$

$$s = 1.4 - 1.8$$

- Similar distribution is found for Earth quakes and in simulations of stressed elastic medium, which suggests that magnetar bursts are “star quakes” and may indeed be a self-critical phenomena.

$$\frac{E}{\langle \dot{E} \rangle} \sim 100 g_{50}^{-1} E_{45.5}\ \mathrm{yr}$$

Conclusions:

- A small natal kick might help MWN detectability
- Possible new internal nebula flow structure (for non-ideal low-σ flow)
- X-ray Nebula Size: may be ~ the diffusion dominated cooling length
- Steady-state X-ray emission: **energy balance** ➔ $\dot{E}_{rot}$ is insufficient

$$g = \frac{\langle \dot{E} \rangle}{L_{\rm sd}} > g_{\rm min} = 3.07 \left(\frac{1+\sigma}{\sigma} \right) d_4^3 E_{M,30}^{7/2} f^{7/2}$$

- An alternative **energy source** is needed:
  - magnetar's **dipole** B-field decay is not enough ✘
  - magnetar's **internal** B-field decay is enough ✓
- Energy from the B-field decay may be injected into the MWN via **outflows** associated with **regular busts** or **giant flares**